

Modeling the Structure of Charged Binary Colloidal Dispersions

S. N. Petris,^{*,†} J. Stankovich,^{†,‡} D. Y. C. Chan,[†] and R. H. Ottewill[§]

Particulate Fluids Processing Centre, Department of Mathematics & Statistics, The University of Melbourne, VIC 3010, Australia; and School of Chemistry, Cantock's Close, Bristol University, Bristol BS8 1TS, U.K.

Received October 1, 2002. In Final Form: November 18, 2002

A computationally simple and accurate model is presented for predicting partial structure factors of binary mixtures of electrostatically stabilized colloidal particles. The theory is based on the mean spherical approximation of a binary mixture of hard sphere fluids interacting with a screened Coulomb (Yukawa) potential and a rescaling of the hard sphere sizes of the components. The utility of the approach is tested against data from small-angle neutron scattering experiments and Monte Carlo simulations.

I. Introduction

In recent small-angle neutron scattering (SANS) experiments, Ottewill et al.¹ measured partial structure factors of dispersions containing two types of spherical polystyrene lattices. The dispersions are held at a relatively low background electrolyte concentration, such that the electrostatic repulsion is strong enough to induce significant structure in the system. With the total volume fraction of particles between 2% and 3%, van der Waals attraction is negligible and effects due to multiple scattering are not important.

By using the deuterated form of the polymer lattices as one of the components, it is possible to measure individual structure factors between the large or between the small sized particles by using a mixture of D₂O/H₂O in the aqueous dispersion to achieve contrast matching and to make one of the species "invisible" to the neutrons. The mixed structure factor between the large and small particles can then be deduced by additional measurements. However, as we shall see, the experimental uncertainties in the mixed structure factor seem to be high and it requires further experimental refinement.

Lutterbach et al.^{2,3} have since presented SANS measurements for a two-component dispersion of highly charged polystyrene (PS) and perfluorinated (PFA) particles at higher volume fractions of approximately 9%. They compared their partial structure factor measurements between the colloidal particles with theoretical predictions from the hypernetted chain (HNC) integral equation and found good agreement.

The structural properties of a colloidal dispersion can be determined by Monte Carlo (MC) simulation, and within statistical uncertainty, it provides an exact answer for the given model. However, this approach is highly resource consuming, and the time needed to complete the simulations can be quite substantial, particularly for highly

charged systems. Therefore, it is desirable to develop a simple but reliable theoretical approximation to determine the structural properties of these systems. Svensson and Jönsson⁴ have tested the RMSA model against Monte Carlo simulations for one-component systems, and they found good agreement for low surface charge densities and volume fractions, provided that the supporting electrolyte is monovalent. In this paper, we present a computationally simple and accurate model based on the rescaled mean spherical approximation (RMSA) for predicting partial structure factors of charged binary colloidal dispersions. The utility of the approach is also tested against SANS data and Monte Carlo simulations.

II. Experimental Details and Pair Potentials

The experimental details regarding the SANS experiments are given elsewhere,¹ we simply summarize the main features. The dispersion consisted of two types of spherical polystyrene lattices, and the size ratio of the particles was 3:1. The volume fraction of the larger (*L*) particles was held constant, while the volume fraction of the smaller (*S*) particles was varied to give small/large (*N_S/N_L*) number ratios of 9 and 15. The total volume fraction was kept low to reduce the effects of multiple neutron scattering—such effects were ignored in the determination of the partial structure factors. Systems with only one of the components present were also studied by SANS, photocorrelation spectroscopy, and transmission electron microscopy to determine particle size and interaction parameters. The physical parameters of the system are given in Table 1.

At an added univalent salt concentration of 6×10^{-5} M, the counterions from the dissociation of surface groups on the particles make a negligible contribution to the Debye screening length in the aqueous medium.^{5,6} The inverse Debye length, κ , for the system can be taken to be

$$\kappa^2 = \frac{2ne^2}{\epsilon\epsilon_0kT} \quad (1)$$

where *e* is the proton charge, *n* is the number concentration of the added salt, ϵ is the relative permittivity of the

* E-mail: S.Petris@ms.unimelb.edu.au.

† The University of Melbourne.

‡ Current address: Menzies Centre for Population Health Research, University of Tasmania, GPO Box 252-23, Hobart 7001, Australia.

§ Bristol University.

(1) Ottewill, R. H.; Hanley, H. J. M.; Rennie, A. R.; Straty, G. C. *Langmuir* **1995**, *11*, 3757.

(2) Lutterbach, N.; Versmold, H.; Reus, V.; Belloni, L.; Zemb, T. *Langmuir* **1999**, *15*, 337.

(3) Lutterbach, N.; Versmold, H.; Reus, V.; Belloni, L.; Zemb, T.; Lindner, P. *Langmuir* **1999**, *15*, 345.

(4) Svensson, B.; Jonsson, B. *Mol. Phys.* **1983**, *50*, 489.

(5) Beresford-Smith, B.; Chan, D. Y. C. *Chem. Phys. Lett.* **1982**, *92*, 474.

(6) Beresford-Smith, B.; Chan, D. Y. C.; Mitchell, D. J. *Colloid Interface Sci.* **1985**, *105*, 216.

Table 1. Composition of Binary Mixtures

| system | radius, a (Å) | vol fraction, ϕ (%) | number ratio (N_S/N_L) |
|-----------|-----------------|--------------------------|----------------------------|
| large (L) | 510 | 2.1 | |
| small (S) | 170 | 0.7, 1.1 | 9, 15 |

aqueous suspension, ϵ_0 is the permittivity of free space, k is Boltzmann's constant, and T is the absolute temperature. At 6×10^{-5} M of added NaCl, the Debye length is $\kappa^{-1} = 390$ Å, so that the scaled particle radii are of order unity:

$$\kappa a_L = 1.3 \quad \kappa a_S = 0.44 \quad (2)$$

To obtain an estimate of the mean separation between particles, let us consider the small/large number ratio (N_S/N_L) of 15 with the volume fraction of large particles $\phi_L = 2\%$. Consider a collection of large particles of radius a_L , arranged in an fcc lattice with a volume fraction of $16\phi_L$. The distance r between the centers of particles is given by

$$\left(\frac{r}{2a_L}\right)^3 = \frac{\pi(3\sqrt{2})}{16\phi_L} \quad \text{or} \quad r = 2.6 a_L = 1326 \text{ Å} \quad (3)$$

where $\pi/(3\sqrt{2}) = 0.74$ is the fcc closed pack volume fraction for spheres. Now if 15 out of every 16 large particles are replaced by small particles of radius $a_S = a_L/3$ and no two large particles are adjacent to one another, then the smallest surface-to-surface distance, h_{\min} , between particles will be between adjacent large and small spheres with

$$h_{\min} = r - a_L - a_S = 1.3a_L = 1.7\kappa^{-1} \approx 660 \text{ Å} \quad (4)$$

At this separation or larger, and for scaled particle radii of order 1, the superposition approximation expression for the double layer interaction energy is expected to be accurate to within 10%.^{7,8} In general, one would expect the typical surface-to-surface separations would be larger than that estimated in eq 4 and would therefore make the superposition approximation even more accurate. Thus, for modeling the structure of these binary colloidal dispersions, we used the following superposition representation⁹ for the repulsive electrical double interaction between the particles belonging to species $\alpha, \beta = L, S$, at a separation r , between their centers

$$U_{\alpha\beta}(r) = \frac{4\pi\epsilon\epsilon_0}{e^2} \frac{a_\alpha e\Psi_\alpha \exp(\kappa a_\alpha)}{kT} \frac{a_\beta e\Psi_\beta \exp(\kappa a_\beta)}{kT} \frac{\exp(-\kappa r)}{r}, \quad r > \sigma_{\alpha\beta} \quad (5)$$

where $\sigma_{\alpha\beta} = a_\alpha + a_\beta$ is the mean diameter. The parameters Ψ_α and Ψ_β are coefficients that characterize the asymptotic screened Coulomb form of the potential profile from a single particle and are not necessarily the actual surface potentials of the particles.

III. Theory

A. Structure Factors and Ornstein–Zernike Equation for Binary Mixtures. The structure of a binary colloidal mixture can be quantified by means of radial distribution functions $g_{\alpha\beta}(r)$ which measure the relative density of a particle of type β at a distance r from a particle of type α . The total correlation functions $h_{\alpha\beta}(r) = g_{\alpha\beta}(r) - 1$ can be calculated directly from computer simulations or from liquid state theory by solving the Ornstein–Zernike (OZ) equation, which relates total correlation functions $h_{\alpha\beta}(r)$ to direct correlation functions $c_{\alpha\beta}(r)$

$$h_{\alpha\beta}(\mathbf{r}) = c_{\alpha\beta}(\mathbf{r}) + \sum_\gamma n_\gamma \int c_{\alpha\gamma}(\mathbf{r}') n_\gamma h_{\gamma\beta}(\mathbf{r} - \mathbf{r}') d\mathbf{r}' \quad (6)$$

where n_γ is the bulk number density of species γ . The three partial structure factors in the binary mixture, $S_{LL}(k)$, $S_{LS}(k)$, and $S_{SS}(k)$, are obtained from SANS experiments, and these are simply the Fourier transforms of the total correlation functions $h_{\alpha\beta}(r)$

$$\mathbf{S}_{\alpha\beta}(k) = \delta_{\alpha\beta} + \frac{4\pi(n_\alpha n_\beta)^{1/2}}{k} \int_0^\infty r h_{\alpha\beta}(r) \sin(kr) dr \quad (7)$$

where $\delta_{\alpha\beta}$ is the Kronecker delta function (1 if $\alpha = \beta$ and 0 otherwise), n_α is the number density (N_α/V), and k is the wavenumber. We can proceed formally by defining the Fourier transforms

$$\tilde{\mathbf{H}}_{\alpha\beta}(k) = (n_\alpha n_\beta)^{1/2} \int h_{\alpha\beta}(r) \exp[i\mathbf{k}\cdot\mathbf{r}] d\mathbf{r} \quad (8)$$

$$\tilde{\mathbf{C}}_{\alpha\beta}(k) = (n_\alpha n_\beta)^{1/2} \int c_{\alpha\beta}(r) \exp[i\mathbf{k}\cdot\mathbf{r}] d\mathbf{r}$$

so that eq 6 can be written in matrix form

$$[\mathbf{I} - \tilde{\mathbf{C}}(k)][\mathbf{I} + \tilde{\mathbf{H}}(k)] = \mathbf{I} \quad (9)$$

where the components of the 2×2 matrixes $\tilde{\mathbf{H}}(k)$ and $\tilde{\mathbf{C}}(k)$ are the functions $\tilde{\mathbf{H}}_{\alpha\beta}(k)$ and $\tilde{\mathbf{C}}_{\alpha\beta}(k)$ and \mathbf{I} is the identity matrix. A formal solution¹⁰ of eq 9 can be expressed in terms of an auxiliary matrix $\tilde{\mathbf{Q}}(k)$ whereby $\tilde{\mathbf{C}}(k)$ is factorized into the form

$$\mathbf{I} - \tilde{\mathbf{C}}(k) = \tilde{\mathbf{Q}}(k)[\tilde{\mathbf{Q}}(-k)]^T \quad (10)$$

where $\tilde{\mathbf{Q}}(k)$ have the required analytic properties. Then the structure factor matrix becomes

$$\mathbf{S}(k) = \mathbf{I} + \tilde{\mathbf{H}}(k) = [\mathbf{I} - \tilde{\mathbf{C}}(k)]^{-1} = ([\tilde{\mathbf{Q}}(-k)]^T)^{-1} (\tilde{\mathbf{Q}}(k))^{-1} \quad (11)$$

From the general result in eq 11, it is possible to deduce a general inequality¹¹ (see Appendix)

$$[\mathbf{S}_{LS}(k)]^2 \leq \mathbf{S}_{LL}(k) \mathbf{S}_{SS}(k) \quad (12)$$

which must hold for all wavenumbers between the three partial structure factors. This general inequality can be useful in determining the internal consistency or accuracy of experimental results.

B. Rescaled Mean Spherical Approximation. To solve the Ornstein–Zernike equation (eq 6) for the total correlation functions $h_{\alpha\beta}(r)$ or the structure factors $S_{\alpha\beta}(k)$, an additional closure relation involving the direct correlation $c_{\alpha\beta}(r)$ is required. This closure condition is in

(7) Glendinning, A. B.; Russel, W. B. *J. Colloid Interface Sci.* **1983**, *93*, 95.

(8) Sader, J. E.; Carnie, S. L.; Chan, D. Y. C. *J. Colloid Interface Sci.* **1995**, *171*, 46.

(9) Bell, G. M.; Levine, S.; McCartney, L. N. *J. Colloid Interface Sci.* **1970**, *33*, 335.

(10) Baxter, R. J. *J. Chem. Phys.* **1970**, *52*, 4559.

(11) Bartlett, P.; Ottewill, R. H. *J. Chem. Phys.* **1992**, *96*, 3306.

general an approximation. For particles interacting via a repulsive screened Coulomb or Yukawa potential as in eq 5, the mean spherical approximation (MSA) is given by the conditions

$$\begin{cases} h_{\alpha\beta}(r) = -1, & r < \sigma_{\alpha\beta} \\ c_{\alpha\beta}(r) = -\frac{U_{\alpha\beta}^{\text{eff}}(r)}{kT}, & r > \sigma_{\alpha\beta} \end{cases} \quad (13)$$

and affords an analytic solution that is particularly useful if it is needed to explore a large range of parameter space.

For repulsive screened Coulomb potentials at low volume fractions, the MSA yields unphysical, negative values for the radial distribution functions¹² $g_{\alpha\beta}(r)$ for separations near contact. However, Hansen and Hayter¹³ suggested a heuristic approach based on increasing or rescaling the hard core size of the colloids without altering the form of the repulsive potential outside the hard core. In this approach, the particle size is increased until the radial distribution functions cease to be negative. This turns out to be a remarkably accurate method of obtaining the structure factors for systems of one-component particles with repulsive Yukawa interactions, and it is called the rescaled mean spherical approximation (RMSA). Ginoza¹⁴ provides a method of solving eq 6 with the Yukawa closure

$$\begin{cases} h_{\alpha\beta}(r) = -1, & r < \sigma_{\alpha\beta} \\ c_{\alpha\beta}(r) = Kd_{\alpha}d_{\beta}\frac{\exp(-zr)}{r}, & r > \sigma_{\alpha\beta} \end{cases} \quad (14)$$

where K , z , and d_{α} are constants. Ginoza's solution builds on previous work by Baxter¹⁰ and Blum and Høye.¹⁵ Substituting the superposition approximation (eq 5) into the MSA (eq 14) gives $c_{\alpha\beta}(r)$ in the required form (eq 14), with

$$\begin{aligned} K &= -\frac{4\pi\epsilon kT}{e^2}, \\ d_{\alpha} &= a_{\alpha}\frac{e\Psi}{kT}\exp(\kappa a_{\alpha}), \\ z &= \kappa \end{aligned} \quad (15)$$

It is worth emphasizing that Ginoza's solution requires the prefactor of $c_{\alpha\beta}(r)$ in eq 14 to be factorizable into α - and β -dependent components. The solution would be more complicated if $c_{\alpha\beta}(r)$ could only be expressed in the more general form

$$c_{\alpha\beta}(r) = K_{\alpha\beta}\frac{\exp(-zr)}{r} \quad (16)$$

C. Rescaling. Once Ginoza's solution has been used to calculate the partial structure factors $S_{\alpha\beta}(k)$, radial distribution functions $g_{\alpha\beta}(r)$ can be found by

$$g_{\alpha\beta}(r) = 1 + \frac{1}{2\pi^2(n_{\alpha}n_{\beta})^{1/2}}\int_0^{\infty}[S_{\alpha\beta}(k) - \delta_{\alpha\beta}]k\sin(kr)dr \quad (17)$$

In Ginoza's solution, the contact value $g_{\alpha\beta}(\sigma_{\alpha\beta}^+)$ can also be calculated directly, without resorting to Fourier

Table 2. Key Parameters for RMSA Calculations Plotted in Figures 1 and 2

| | 9:1 (Figure 1) | 15:1 (Figure 2) |
|--|-------------------------------------|-------------------------------------|
| surface potentials yielding the best fit to experiment | $\Psi_L = 21$ mV $\Psi_S = 7$ mV | $\Psi_L = 21$ mV $\Psi_S = 7$ mV |
| RMSA scale factors | $s_L^* = 1.67$ $s_S^* = 1$ | $s_L^* = 1.63$ $s_S^* = 1$ |
| effective radii | $a_L^* = 852$ Å $a_S^* = 168$ Å | $a_L^* = 831$ Å $a_S^* = 168$ Å |

transforms. This contact value is the limiting value of $g_{\alpha\beta}(r)$ as r approaches $\sigma_{\alpha\beta}$ from above. Since $g_{\alpha\beta}(r)$ is zero for all $r < \sigma_{\alpha\beta}$, $g_{\alpha\beta}(r)$ is discontinuous at $r = \sigma_{\alpha\beta}$ if the contact value is nonzero.

Hayter and Penfold¹² have previously derived a method of calculating structure factors $S(k)$ and radial distribution functions $g(r)$ for one-component systems, analogous to Ginoza's. Subsequently, Hansen and Hayter¹³ noted the tendency of $g(\sigma^+)$ to become negative under the MSA closure. To overcome this problem, they proposed a rescaled mean spherical approximation (RMSA) model in which particles have an effective hard sphere radius larger than their true radius by some scale factor $s > 1$, without changing the form of the pair potential. Let $g(s; r)$ denote the radial distribution function $g(r)$ found by solving the OZ equation with scale factor s . Then, since we would expect the rescaled contact value $g(s; \sigma^+)$ to increase monotonically as a function of s , there should be a unique s^* for which $g(s^*; \sigma^+) = 0$. An iteration scheme is required to find s^* .

For our binary mixtures, we must ensure that three distribution functions are non-negative at contact, while we only have two adjustable effective diameters at our disposal. Let $g_{\alpha\beta}(s_L, s_S; r)$ denote the radial distribution functions found by solving the OZ equation with the large and small particle radii scaled by factors s_L and s_S . We searched numerically for a pair of scale factors (s_L^*, s_S^*) such that the rescaled contact values $g_{LL}(s_L^*, s_S^*; s_L^*\sigma_L)$ and $g_{SS}(s_L^*, s_S^*; s_S^*\sigma_S)$ are zero. As in the one-component case, we expect the root (s_L^*, s_S^*) to be unique, since it is likely that $g_{LL}(s_L, s_S; s_L\sigma_L)$ and $g_{SS}(s_L, s_S; s_S\sigma_S)$ both increase monotonically as functions of both s_L and s_S .

Once the root (s_L^*, s_S^*) is found, we have to check that the contact value of the third pair distribution function $g_{LS}(s_L^*, s_S^*; (s_L^*\sigma_L + s_S^*\sigma_S)/2)$ is also non-negative, which turned out to be true for all the cases we considered. Some typical scale factors (s_L^*, s_S^*) are given in Table 2, and they tend to increase as the surface potentials are increased. In some cases for low surface potentials rescaling is not required.

IV. Monte Carlo Simulation

As well as comparing the RMSA results with SANS experiments, RMSA predictions were tested against Monte Carlo (MC) simulations. The MC simulations were carried out using the canonical ensemble with 200 large particles and 9×200 or 15×200 small particles enclosed in a cubic box with periodic boundary conditions. The particles interacted using the pair potential in eq 5, which is also used in the RMSA model. The simulations involved 2000 MC passes (attempted moves per particle) for equilibration and then 40 000 passes for production runs. All the simulations were performed using the integrated Monte Carlo/molecular dynamics/Brownian dynamics simulation package MOLSIM.¹⁶ Radial distribution functions $g_{\alpha\beta}(r)$ were calculated by averaging over all but the first 2000 cycles. From the expressions for $g_{\alpha\beta}(r)$, partial structure

(12) Hayter, J. B.; Penfold, J. *Mol. Phys.* **1981**, *42*, 109.

(13) Hansen, J. P.; Hayter, J. B. *Mol. Phys.* **1982**, *46*, 651.

(14) Ginoza, M. *J. Phys. Soc. Jpn.* **1986**, *55*, 95.

(15) Blum, L.; Høye, J. S. *J. Stat. Phys.* **1978**, *19*, 317.

(16) Linse, P. *MOLSIM*; Lund University: Sweden, 2002.

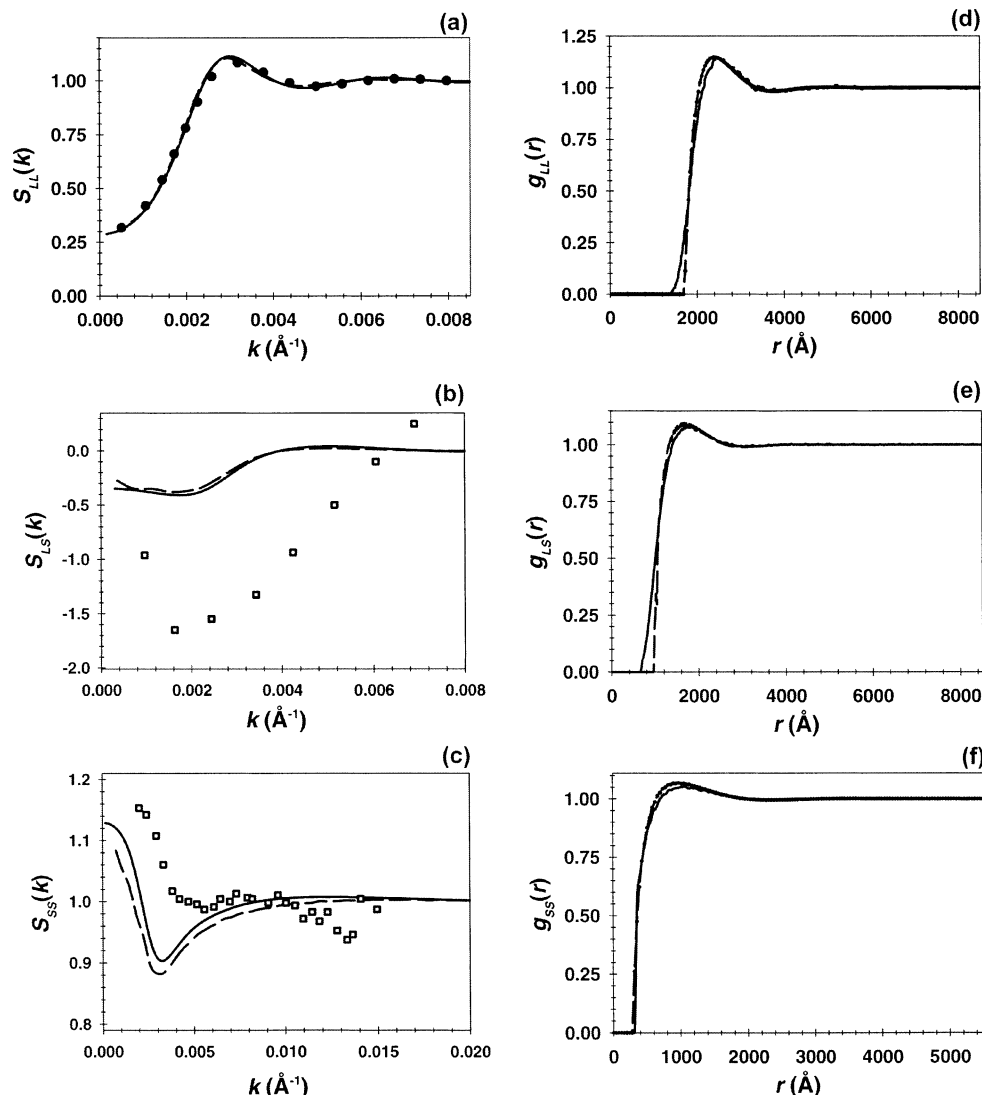


Figure 1. Partial structure factors (a) $S_{LL}(k)$, (b) $S_{LS}(k)$, and (c) $S_{SS}(k)$ and radial distribution functions (d) $g_{LL}(r)$, (e) $g_{LS}(r)$, and (f) $g_{SS}(r)$ for mixtures of large (L) and small (S) colloids with the number ratio $N_S/N_L = 9$. The points are the experimental results of Ottewill et al.,¹ the RMSA (dashed lines), and the MC simulation (continuous lines). The points in part a come from the fitted experimental curve for $S_{LL}(k)$ presented by Ottewill et al.,¹ while the points in parts b and c are their actual experimental data.

factors $S_{\alpha\beta}(k)$ were found by evaluating eq 7 with a fast Fourier transform.

V. Results

A. Partial Structure Factors. Ottewill et al.¹ fitted their one-component structure factor measurements using the RMSA procedure of Hayter and Hansen, and from these fits, they estimated the surface potentials of the large and small particles to be $\Psi_L = 15$ mV and $\Psi_S = 8$ mV. We found that Ginoza's RMSA solution gave the best fit to the binary system measurements if the surface potentials used in eq 5 were $\Psi_L = 21$ mV and $\Psi_S = 7$ mV. With such a low potential on the small particle, no rescaling was required, while the large particles were rescaled for both cases. Some key parameters for the RMSA calculations are given in Table 2.

In Figure 1, the experimental partial structure factors are compared with the RMSA and MC simulation results for the number ratio of 9. Figure 1a shows the large/large partial structure factors, and it illustrates that $S_{LL}(k)$ values from the RMSA, experiment, and MC simulation compare very well, as all three curves are almost identical. $S_{LL}(k)$ has the typical shape for a "fluidlike" structure with repulsive forces acting between the particles.

The greatest discrepancy between experiment, theory, and simulation is for the large/small partial structure factor $S_{LS}(k)$, which is shown in Figure 1b. The RMSA and MC simulation curves are in very close agreement with each other, but the experimental values for $S_{LS}(k)$ are much larger in magnitude for low k . Ottewill et al. pointed out that the experimental values for $S_{LS}(k)$ were larger in magnitude than expected and noted that these measurements were considerably more difficult to obtain accurately than the measurements of $S_{LL}(k)$ and $S_{SS}(k)$. Indeed, it seems likely that there was some error in the measurement of $S_{LS}(k)$, since partial structure factors should satisfy the inequality¹¹ in eq 12 for all k (see Appendix). The experimental results appear to be inconsistent with the inequality, since the values of $S_{LS}(k)$ can be much less than -1 but the values of $S_{LL}(k)$ and $S_{SS}(k)$ are rarely much greater than 1.

The small/small partial structure factors $S_{SS}(k)$ are compared in Figure 1c. The RMSA and MC simulation curves are in very close agreement with each other, and they are in qualitative agreement with the experimental data. The first minimum in $S_{SS}(k)$ is fairly weak in the experimental data, and it is much more prominent in the RMSA and MC curves. Ottewill et al.¹ were somewhat

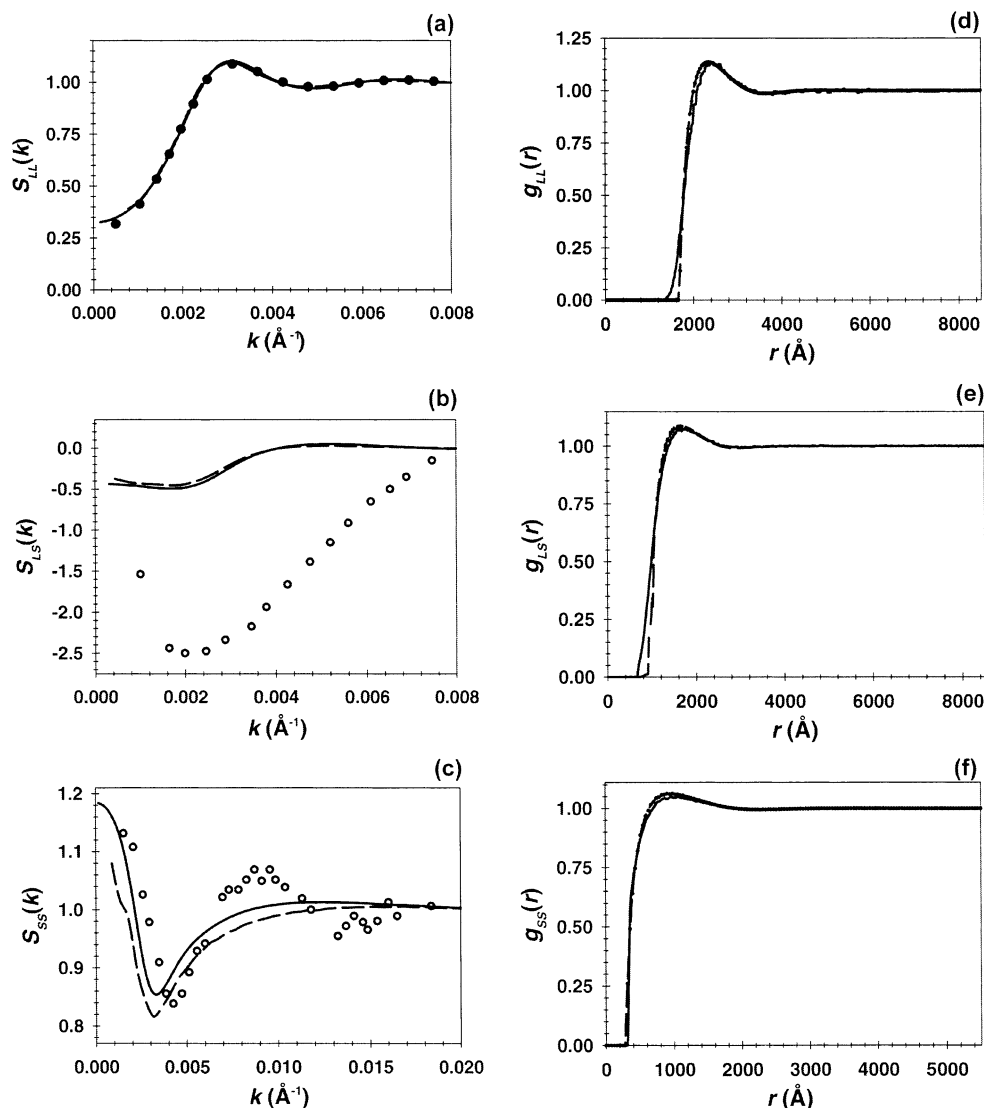


Figure 2. Partial structure factors (a) $S_{LL}(k)$, (b) $S_{LS}(k)$, and (c) $S_{SS}(k)$ and radial distribution functions (d) $g_{LL}(r)$, (e) $g_{LS}(r)$, and (f) $g_{SS}(r)$ for mixtures of large (L) and small (S) colloids with the number ratio $N_S/N_L = 15$. The points are the experimental results of Ottewill et al.,¹ the RMSA (dashed lines), and the MC simulation (continuous lines). The points in part a come from the fitted experimental curve for $S_{LL}(k)$ presented by Ottewill et al.,¹ while the points in parts b and c are their actual experimental data.

surprised by the considerable rise in $S_{SS}(k)$ at low k , indicating a long-range correlation between the small particles due to depletion effects which cause the small particles to cluster. Interestingly, this characteristic rise in $S_{SS}(k)$ was also evident in the RMSA and MC results.

In Figure 2, the experimental partial structure factors are compared with the RMSA and MC simulation results for the number ratio of 15. Once again, the large/large partial structure factors (Figure 2a) from experiment, RMSA, and MC simulation compare very well, as all three curves are almost identical. Within experimental error, the values of $S_{LL}(k)$ for both number ratios appear to be very close in form and in the positions of the peaks.¹ This observation is also the case for the RMSA and MC simulations. There was very little change in $S_{LL}(k)$ as the number ratio was increased from 9 to 15; thus, it seems that the small particles do not greatly affect the repulsive electrostatic interaction between the large particles.

Once again there was a significant discrepancy between theoretical and experimental values of $S_{LS}(k)$ in Figure 2b. The RMSA and MC simulation curves are in very close agreement with each other, but the experimental values of $S_{LS}(k)$ seem improbably large in magnitude and again violate the partial structure factor inequality in eq 12.

The small/small partial structure factors $S_{SS}(k)$ are compared in Figure 2c. The RMSA and MC simulation $S_{SS}(k)$ curves are in very close agreement with each other, and they are in qualitative agreement with the experimental values. The position and depth of the first minimum in $S_{SS}(k)$ are approximately the same in theory and experiment (around 0.004 \AA^{-1} and 0.82, respectively); however, the observed structure for larger k seen in the experiments is not as prominent in the RMSA results.

B. Radial Distribution Functions. The radial distribution functions calculated using the RMSA model and MC simulation are compared in Figures 1d–f and 2d–f, for the number ratios of 9 and 15, respectively. No experimental curves are shown because the data were not obtained over a large enough range of k values to yield smooth and accurate radial distribution functions.

The RMSA and MC radial distribution functions display the typical characteristics for a fluid, which is a pronounced first maximum at some interparticle distance, followed by successive minima and maxima of reduced amplitude. The amplitudes and positions of the maxima and minima from theory and simulation are in very close agreement. However, in the Monte Carlo simulations, there is some possibility that the particles may approach one another

to within a distance slightly smaller than their effective diameters allow in the RMSA model.

Svensson and Jönsson⁴ commented that distribution functions calculated with a screened Coulomb potential are virtually identical to HNC results for a system with both colloids and counterions interacting via a Coulombic potential. Lutterbach et al.^{2,3} solved the HNC equation with a screened Coulomb potential to compare with their experimental partial structure factors. We thus compared our RMSA predictions for the two-component dispersion of Lutterbach et al.^{2,3} and found them to be virtually identical to their HNC predictions. Recently, we have developed a technique called the boot-strap Poisson Boltzmann (BSPB) theory¹⁷ to determine all the pair distribution functions for a system of colloids and explicit counterions.

VI. Conclusions

We have used Ginoza's RMSA solution of the OZ equation to calculate partial structure factors for a binary mixture of charged colloidal particles. The RMSA model can reproduce the most significant features of the SANS experiments conducted by Ottewill et al.:¹ the increase in the small/small partial structure factor $S_{SS}(k)$ as k approaches zero and the fluidlike large/large partial structure factor $S_{LL}(k)$. The RMSA also agrees with the observation of Ottewill et al.¹ that the arrangement of the larger particles is not affected significantly by the presence of the smaller particles. However, analysis suggests that the experimental measurements of $S_{LS}(k)$ are inaccurate because some of the values violate an inequality between the partial structure factors. Following the example of Bartlett and Ottewill¹¹ in their SANS studies of binary colloidal crystals, it would be interesting to see whether extra SANS measurements at other scattering densities yield more information about this cross-particle correlation. The RMSA results were also found to compare very favorably with Monte Carlo simulations of particles interacting via a Yukawa potential.

Acknowledgment. This research is supported by the Australian Research Council and the Particulate Fluids Processing Centre at the University of Melbourne.

Appendix: Inequality Relating the Partial Structure Factors

The inequality (eq 12) relating the three partial structure factors for our binary system was deduced by Bartlett and Ottewill¹¹ by expressing the scattered intensity $I(k)$ of a neutron beam in terms of the three structure factors and noting that $I(k)$ must be positive for all k . The inequality can also be deduced from the factorization (eq 11) of the partial structure factor matrix $\mathbf{S}(k)$ in terms of the matrix $\tilde{\mathbf{Q}}(k)$. $\tilde{\mathbf{Q}}(k)$ is expressed in terms of scalar functions $\tilde{Q}_{\alpha\beta}(k)$, which can be written in terms of a function $Q_{\alpha\beta}(r)$ (eq 3 in ref 14):

$$\tilde{Q}_{\alpha\beta}(k) = \int_{\lambda_{\alpha\beta}}^{\infty} \exp(ikr) Q_{\alpha\beta}(r) dr \quad (\text{A.1})$$

where $\lambda_{\alpha\beta} = (\sigma_{\alpha} - \sigma_{\beta})/2$. Since the $Q_{\alpha\beta}(r)$ are real, it follows that $\tilde{\mathbf{Q}}(-k)$ is the complex conjugate of $\tilde{\mathbf{Q}}(k)$.

For our binary system with components L and S, we can write the matrix $(\tilde{\mathbf{Q}}(-k))^{-1}$ in the form

$$(\tilde{\mathbf{Q}}(-k))^{-1} = \begin{pmatrix} x_{LL}(k) + iy_{LL}(k) & x_{LS}(k) + iy_{LS}(k) \\ x_{LL}(k) + iy_{LL}(k) & x_{SS}(k) + iy_{SS}(k) \end{pmatrix} \quad (\text{A.2})$$

where the $x_{\alpha\beta}$ and $y_{\alpha\beta}$ are real functions. Substituting eq A.2 into eq 11 and using the fact that $\tilde{\mathbf{Q}}(-k)$ and $\tilde{\mathbf{Q}}(k)$ are conjugates gives

$$\begin{aligned} \mathbf{S}(k) &= \begin{pmatrix} S_{LL}(k) & S_{LS}(k) \\ S_{LS}(k) & S_{SS}(k) \end{pmatrix} \\ &= \begin{pmatrix} (x_{LL})^2 + (y_{LL})^2 + (x_{LS})^2 + (y_{LS})^2 & x_{LL}x_{LS} + y_{LL}y_{LS} + x_{SL}x_{SS} + y_{SL}y_{SS} \\ x_{LL}x_{LS} + y_{LL}y_{LS} + x_{SL}x_{SS} + y_{SL}y_{SS} & (x_{LS})^2 + (y_{LS})^2 + (x_{SS})^2 + (y_{SS})^2 \end{pmatrix} \\ &= \begin{pmatrix} (z_{LL})^2 + (z_{SL})^2 & \mathbf{z}_{LL} \cdot \mathbf{z}_{LS} + \mathbf{z}_{SL} \cdot \mathbf{z}_{SS} \\ \mathbf{z}_{LL} \cdot \mathbf{z}_{LS} + \mathbf{z}_{SL} \cdot \mathbf{z}_{SS} & (z_{LS})^2 + (z_{SS})^2 \end{pmatrix} \end{aligned} \quad (\text{A.3})$$

defining the vector $\mathbf{z}_{AB} = (x_{AB}, y_{AB})$ with magnitude z_{AB} . Note that we have dropped the imaginary component ($x_{LL}y_{LS} + x_{SL}y_{SS} - x_{LS}y_{LL} - x_{SS}y_{SL}$) of S_{LS} , since S_{LS} must be real.

Now from eq A.3 we have that

$$\begin{aligned} (S_{LS})^2 &= (\mathbf{z}_{LL} \cdot \mathbf{z}_{LS})^2 + 2(\mathbf{z}_{LL} \cdot \mathbf{z}_{LS})(\mathbf{z}_{SL} \cdot \mathbf{z}_{SS}) + (\mathbf{z}_{SL} \cdot \mathbf{z}_{SS})^2 \\ &\leq (\mathbf{z}_{LL} \cdot \mathbf{z}_{LS})^2 + 2|\mathbf{z}_{LL} \cdot \mathbf{z}_{LS}||\mathbf{z}_{SL} \cdot \mathbf{z}_{SS}| + (\mathbf{z}_{SL} \cdot \mathbf{z}_{SS})^2 \\ &\leq (z_{LL})^2(z_{LS})^2 + 2(z_{LL}z_{LS})(z_{SL}z_{SS}) + (z_{SL})^2(z_{SS})^2 \end{aligned} \quad (\text{A.4})$$

using the Cauchy–Schwarz inequality to obtain the last line. The middle term on the last line $2(z_{LL}z_{LS})(z_{SL}z_{SS})$ is less than $(z_{LL})^2(z_{SS})^2 + (z_{SL})^2(z_{LS})^2$, since

$$(z_{LL})^2(z_{SS})^2 + (z_{SL})^2(z_{LS})^2 - 2(z_{LL}z_{LS})(z_{SL}z_{SS}) = (z_{LL}z_{SS} - z_{SL}z_{LS})^2 \geq 0 \quad (\text{A.5})$$

Thus

$$(S_{LS})^2 \leq (z_{LL})^2(z_{LS})^2 + [(z_{LL})^2(z_{SS})^2 + (z_{SL})^2(z_{LS})^2] + (z_{SL})^2(z_{SS})^2 = S_{LL}(k) S_{SS}(k)$$

as required.

LA026641K

(17) Petris, S. N.; Chan, D. Y. C.; Linse, P. *J. Chem. Phys.*, submitted.